ISMEM 2017
- 2nd International Symposium on Multiscale Experimental Mechanics: Multiscale Fatigue

A novel single actuator test setup for combined loading of wind turbine rotor blade sub-components

Malo Rosemeier[1], Moritz Bätge[1] and Alexandros Antoniou[1]

[1] Divison Structural Components, Fraunhofer Institute for Wind Energy and Energy System Technology IWES, Am Seedeich 45, 27572 Bremerhaven, Germany

e-mail: malo.rosemeier@iwes.fraunhofer.de

Malo Rosemeier M.Sc. in wind energy engineering, Research Associate at Fraunhofer IWES. Research interests: adhesive joints of wind turbine rotor blade structures, model validation of experiments for blades and blade components.

Moritz Bätge Dipl.-Ing. in lightweight design, Research Associate at Fraunhofer IWES. Research interests: mechanical design validation of rotor blades, testing of blade components, methods for testing the next generation of large scale rotor blades.

Abstract

Wind turbine rotor blade sub-component testing (SCT) confines the structural validation to design critical blade parts. SCT can replicate the stress state of the blade structure closer to field conditions than full-scale blade testing. Hence sub-component testing could augment towards increasing the reliability of rotor blade structures. This work presents a novel single actuator test setup for rotor blade sub-components under combined loading. Two different configurations, elaborated for an inboard and an outboard trailing edge sub-component, are compared to assess the scalability. The impact of the structural and geometric sub-component properties, as e. g. the ratio between bending and axial stiffness, on the critical test rig components is identified as a scaling design driver.

1 Introduction

Wind turbine rotor blade sub-component testing (SCT) confines the structural validation to design critical blade parts. These detailed tests can mimic the stress state a blade is exposed to in the field more accurately than full-scale blade tests can [4]. Hence SCT could augment towards increasing the reliability of rotor blade structures.
One of the blade regions most sensitive to fatigue is the trailing edge bond line. In the outboard region of rotor blades the geometry, the design of this bond line and the surrounding structure is relatively continuous along the blade span. Towards the blade root in the inboard region the trailing edge geometry, the surrounding structure and the bond line design is subjected to discontinuities. There are several test setups elaborated for SCT of the outboard trailing [1-3]. However, their applicability on corresponding inboard sub-components is not yet assessed.
Test configurations applied for structural rotor blade full-scale and SCT differ compared to other branches such as aerospace or automotive. Present testing of full-scale rotor blades is conducted with relatively simple setups as described in [4]. While the static test requires multiple shear force introduction points along the blade span to effect a multi-linear bending moment distribution, the fatigue test requires just a single actuator exciting the structure to oscillate in resonance.
Alternative fatigue test methods for full-scale blades propose different excitation strategies, e. g. the excitation of the blade hub introducing a bending moment at the blade root [5].
If it comes to fatigue testing of blade segments or sub-components, various methods differing from the full-scale approach can be found. A novel method [6] arranges the blade segment simply supported at both sides with a single actuator introducing a shear force exciting the structure in resonance. The resulting bending moment distribution along the specimen shows a parabolic shape.
With decreasing scale and mass of the specimen, the corresponding eigenfrequency is increasing drastically. As a consequence fatigue resonance testing of specimens such as trailing edge sub-components is not efficient. Single actuator test rigs were designed to test trailing edge components which mimic the structural response of the full-scale experiment. The specimen is mounted in between two rotating arms hinged on a strong floor while an actuator is connecting these arms [2, 3].
This work presents an alternative single actuator test setup for rotor blade sub-components under combined loading. Two different configurations, elaborated for an inboard and an outboard trailing edge sub-component, are compared to assess the scalability.

2 Test setup

The test setup proposed in this work is designed with a single actuator (Figure 1) allowing the flexible adjustment of combined static and fatigue loading scenarios for blade sub-components, which are either cut out of a full-scale blade or manufactured separately. The shown test setup is not applicable for full cross-sections.
The specimen is glued into load frames at its span-wise edges, which are mounted to ball joints R and T. Joint T is mounted to a stiff wall and joint R is mounted to a vertical beam that is hinged on a strong floor at joint B. The actuator is mounted between another stiff wall (joint C) and the vertical beam (joint D) allowing for a flexible positioning along the height, which makes it possible to operate the actuator in its most efficient position w. r. t. force and displacement.
The concept allows the adjustment of the following parameters: (a) the distance between the axis through ball joints R and T (RT-axis), and the line of centroids z_c' defines the bending moment distribution M along the specimen due to an eccentrically introduced force F, and (b) the superposition of the resulting normal force distribution N and M defines the target strain distribution across the cross-section. This concept is described in detail by Rosemeier et al. [1]. The shape of the bending moment distribution depends on the shape of the line of centroids z_c', which can be influenced by the shape of the specimen's cut along the span or by addition of material or springs connected in parallel to the specimen.
The design critical components of the setup are the shafts of the ball joints R and T, especially when they are subjected to a bending moment introduced via shear force in the global x*y*-plane through joint R, for example, which can be determined by

$$Q_R = \frac{l_r\text{-}l_t}{L} \cdot F$$

where l_r-l_t is the distance between the action lines through the ball joint shafts [1], L is the span-wise distance between the ball joints and F is the axial force introduced into the specimen. For example, with a ratio of $\frac{l_r\text{-}l_t}{L} = \frac{1}{8}$ the allowable axial force F for a ball joint can be reduced by 50 %. This shear force Q_R can be eliminated when the specimen is tilted such that the action line of the introduction and reaction forces at R and T positions, respectively, coincide with the shafts of the ball joint, or in other words if l_r-l_t = 0.
Moreover, another challenge of the test concept is the existence of a rigid body motion about the RT-axis, since, in the ideal case, a ball joint does not constrain the rotational degree of freedom about its shaft axis. Connecting the specimen to the strong wall with springs would reduce the risk of rotation about the RT-axis. In the described setup, however, the specimen is mounted horizontally. Therefore, the gravity load augments the constraint of the rigid body motion.

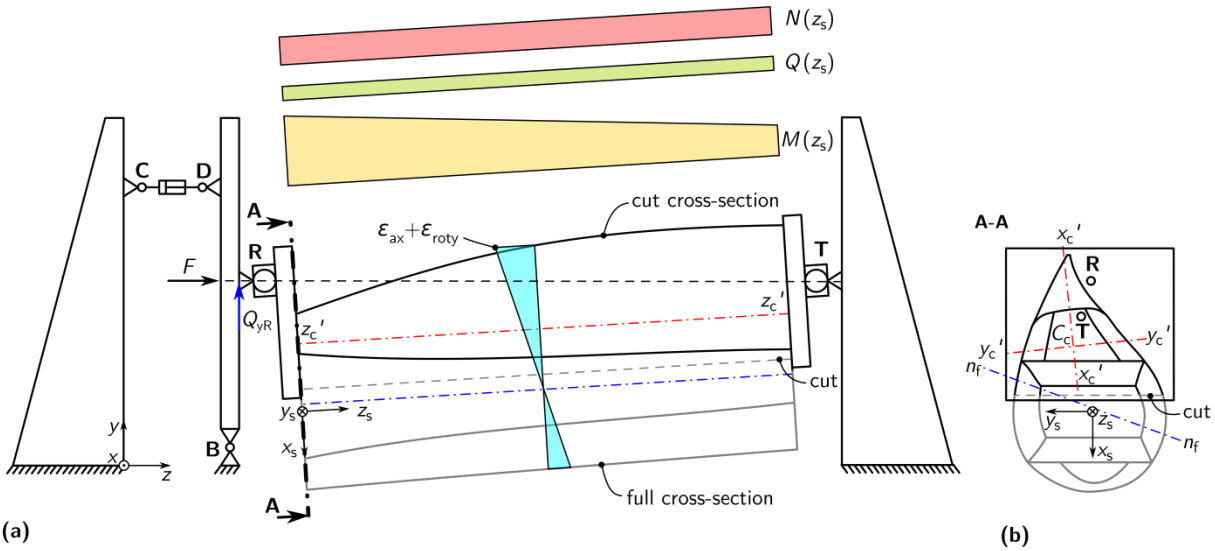

Figure 1: Side view of the setup (a): a segment cut cross-section (black) of a full cross-section (grey) is cut out and clamped between ball joint R and T. Ball joint T is connected to a stiff wall. Ball joint R is connected to vertical beam, which is mounted to a strong floor at hinge B. An adjustable actuator connects the beam at joint D with another stiff wall at joint C. The front view into plane A-A is shown in (b).

3 Methods and Results

The structural response of the suggested test setup is analyzed using the example of a 34 m blade design. An inboard and an outboard trailing edge sub-component of approximately 3 m length were virtually cut out having their target mid cross-sections at 21 % and 71 % blade length, respectively. The segments were further cut in span-wise direction such that only the area of interest remains, in this case the trailing edge cell including one main shear web.

An analytical beam model on the basis of Euler-Bernoulli beam theory [13] was assembled with cross-section properties determined by the Beam Cross Section Analysis Software BECAS [7-10]. Moreover, finite element shell models of the full-scale blade test and the sub-component test setup were implemented in ANSYS APDL [11]. The blade parameterization and input generation for the models was conducted using workflows of the FUSED-Wind framework [12].

The positions of the load introduction points at the specimen edges (R and T in Figure 1) were determined using the analytical model of the full and the cut cross-section. The structural response of the static full-scale leading-to-trailing edge (LTT) load case was chosen as reference.

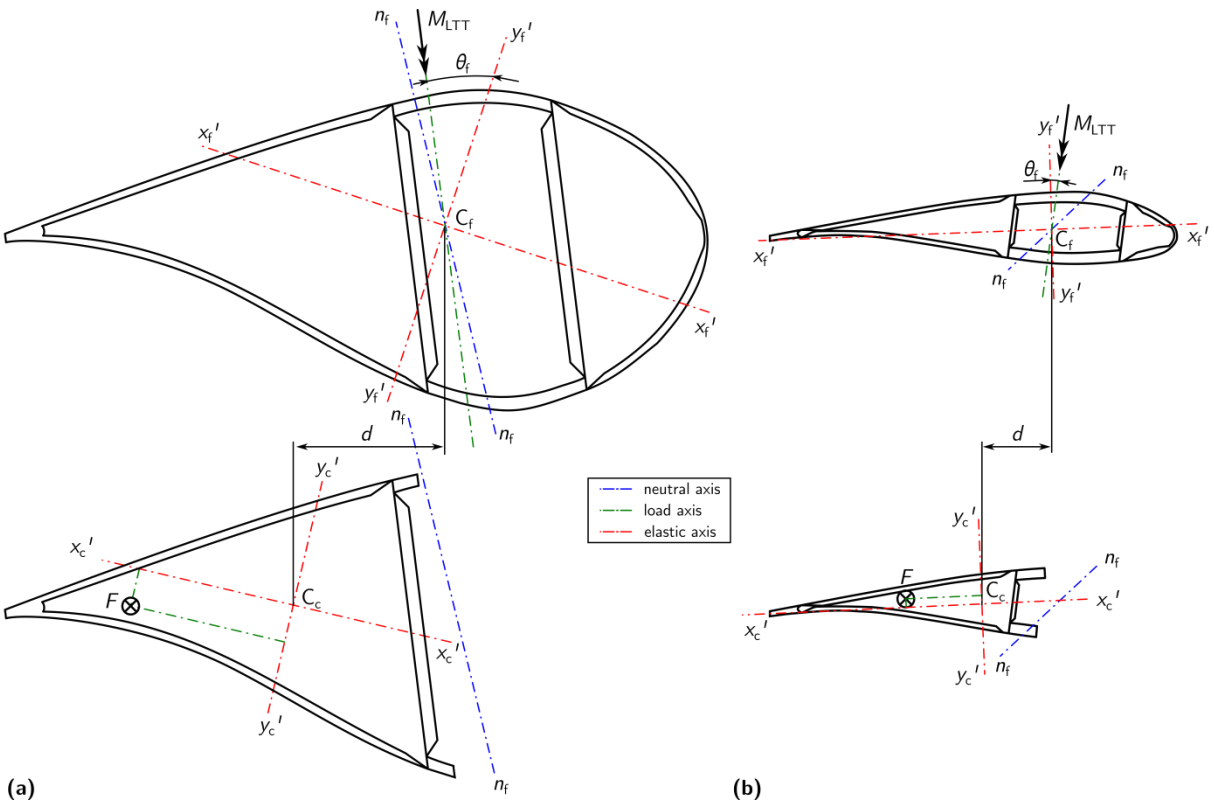

Figure 2: Geometric and structural properties for an inboard (a) and an outboard cross-section (b). The upper figures show the full cross-sections of the blade, whereas the lower figures show the cut cross-sections considered for a sub-component test (SCT). Besides the elastic axes *x*' and *y*' and its centroid *C*, the neutral axis n_f due to the bending moment M_{LTT} of static full-scale leading-to-trailing edge (LTT) load case is highlighted. The axial load introduction point *F* needs to be used in an SCT to reproduce the same neutral axis as in the full-scale LTT load case.

The geometric and structural properties of the inboard and outboard cross-sections are shown in Figure 2. The neutral axis n_f in the full cross-section, determined from the loading of the LTT load case, is replicated by an eccentric axial force *F* in the cut cross-section. Because of the larger inclination angle θ_f between the load axis and the elastic axis y_c', the contribution of the flat-wise bending stiffness $EI_{x'}$ is more prominent for the inboard cross-section compared the outboard cross-section. This becomes more apparent when comparing the cantilever arm components of the eccentricity perpendicular to the elastic axes x_c' and y_c' of the axial force *F* (Figure 2, dash-dotted green axes in lower figures).
The magnitude of the force *F* is influenced by the ratio between the bending stiffness *EI* and axial stiffness *EA* of the specimen, which can also be expressed by the radius of gyration as [14]:

$$r = \sqrt{\frac{EI}{EA}}$$

The flat-wise r_x is larger by a factor of 4.3 while the edge-wise r_y is larger by a factor of 2 when the inboard cross-section is compared to the outboard (Figure 3a). Furthermore, the

chord-wise distance *d* between the centroid of the full and the cut cross-section is also larger by a factor of 2 (Figure 2 and 3b).

Moreover, the force *F* contributes to the actuator work, which is defined as [14]:

$$W = \frac{1}{2} F \cdot \delta$$

where δ is the axial displacement of the joint R. The work required for the inboard cross-section is larger by a factor of 5.8 (Figure 4a). The contribution of *F*, however, is more prominent by a factor of 3.6 for the inboard compared to the outboard cross-section (Figure 4b). Assuming an axial strain amplitude of ε_z = 1000 µm/m for a fatigue test, the ball joints R and T need to resist an axial load amplitude *F* of 404 kN and 113 kN for inboard and outboard cross-section, respectively. Considering the static test load of the LTT load case, the ball joints need to resist an axial ultimate force *F* of 944 kN and 163 kN, respectively.

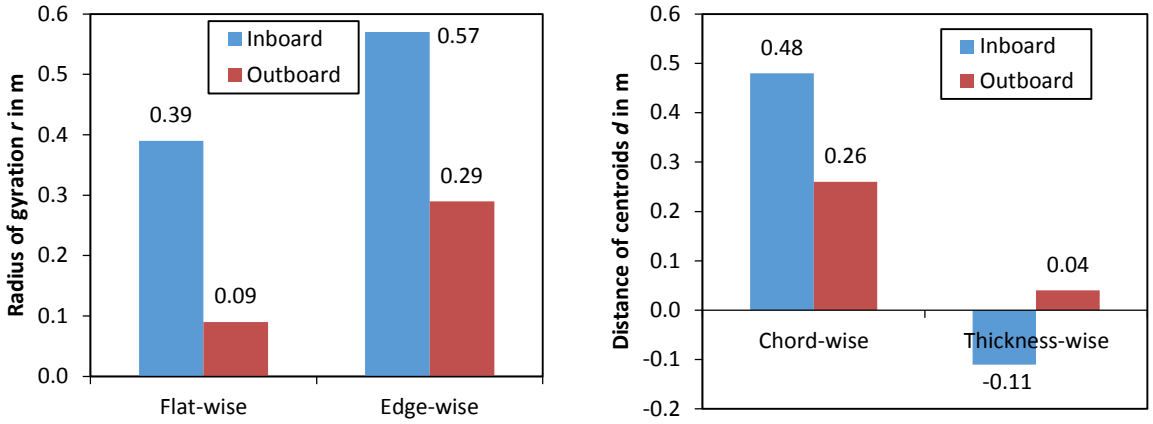

(a) **(b)**

Figure 3: Radii of gyration *r* (a) and distance of the centroids *d* as shown for the chord-wise direction in Figure 2 (b). The inboard cross-section is compared with the outboard cross-section.

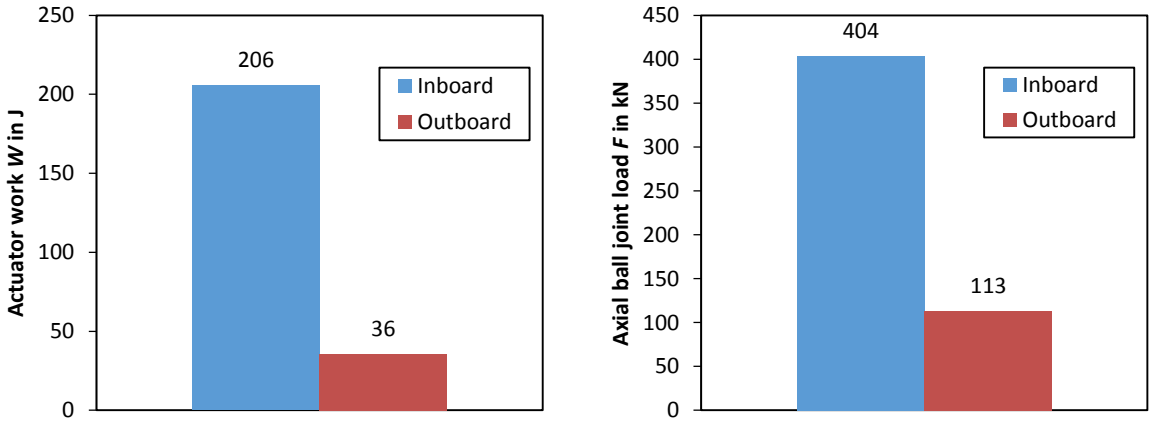

(a) **(b)**

Figure 4: Actuator work *W* required reaching an axial strain level of 1000 µm/m at the trailing edge bond line (a) and resulting axial load *F* at the ball joints (b). The inboard cross-section is compared with the outboard cross-section.

Comparing the structural response of both cross-sections (Figure 5) it is apparent that the target strain distribution is irregular along the specimen's span of the inboard cross-section compared to the outboard cross-section (Figure 6). This is due to the more prominent geometric and structural changes in the inboard blade region, whereas the cross-section at the outboard region can be considered as prismatic extrusion of the target cross-section. Focusing on the axial strain ε_z across the cross-section surface, the analytical models deviate more from the finite element models for the inboard cross-section compared to the outboard (Figure 7).

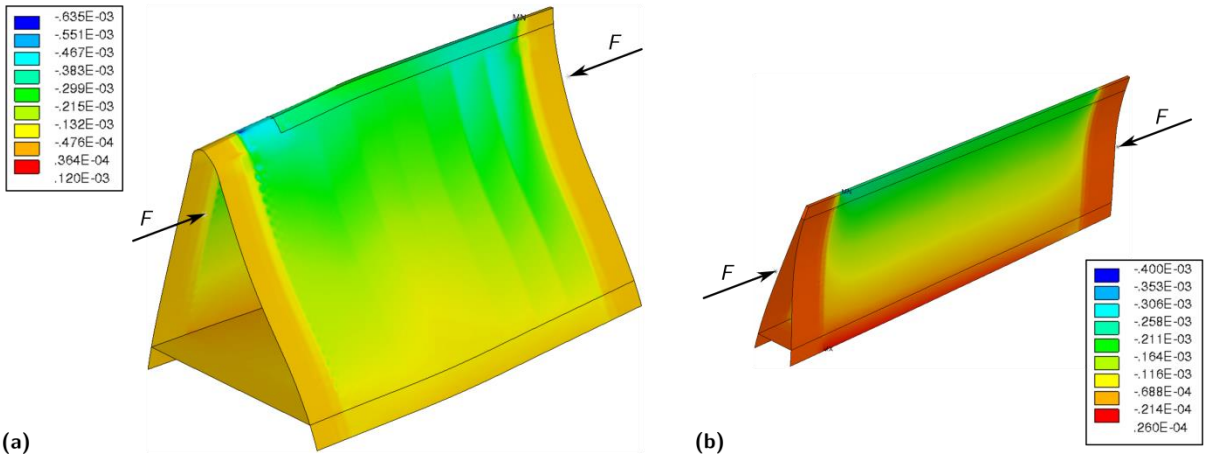

Figure 5: Finite element models of an inboard (a) and an outboard (b) cross-section. The color scale shows the axial strain ε_z at 20 % load level of the final test load of the leading-to-trailing edge (LTT) load case.

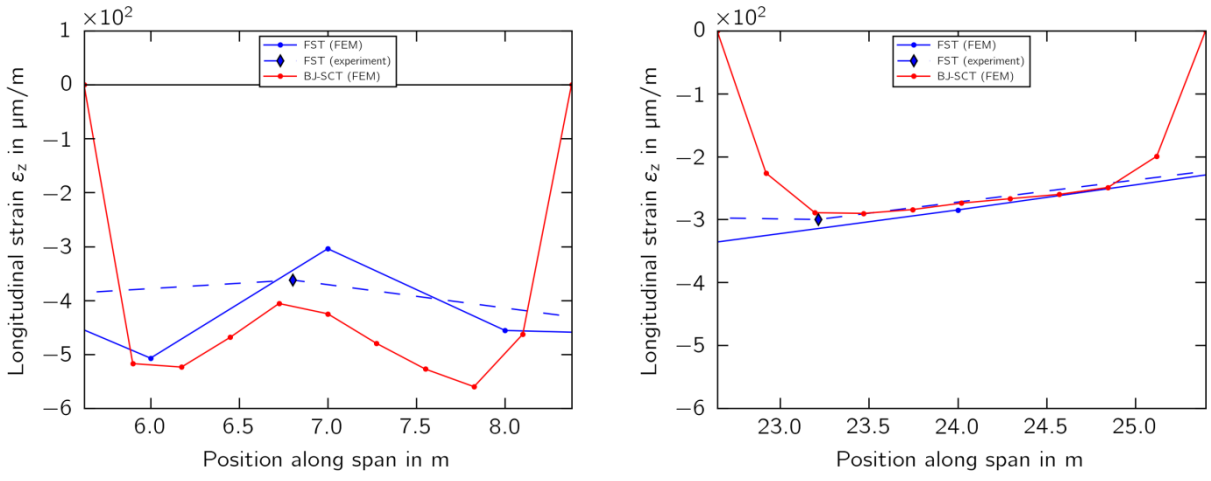

Figure 6: Validation of the full-scale blade (FST) and sub-component (SCT) FE models with the full-scale experiment using the full-scale leading-to-trailing edge (LTT) load case. The longitudinal strain ε_z along the trailing edge bond line at 20 % load level of the final test load is shown for an inboard (a) and an outboard cross-section (b).

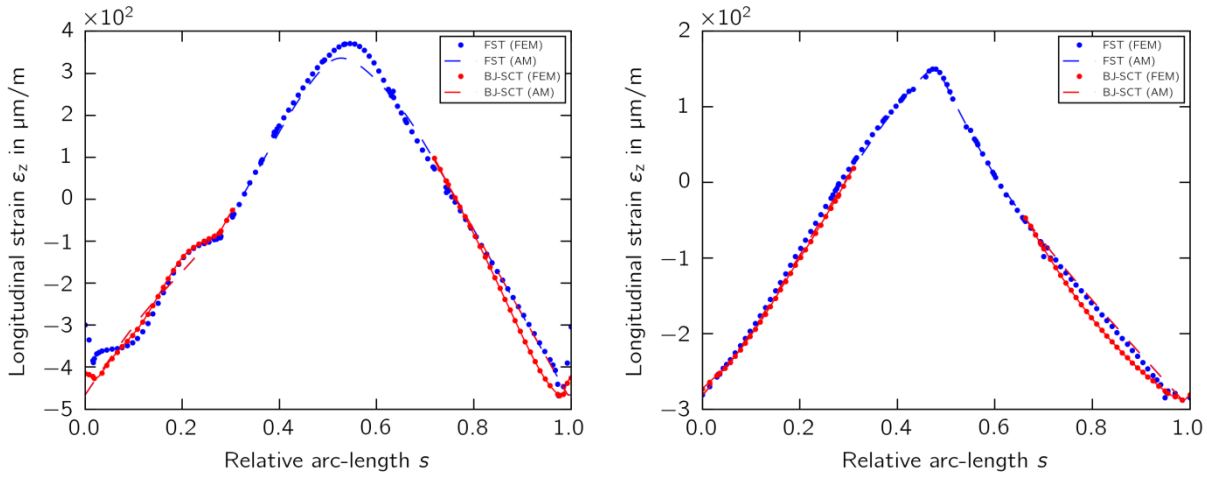

Figure 7: Verification of the sub-component test's (SCT) analytical (AM) and finite element model (FEM) with the full-scale test's (FST) models. The longitudinal strain ε_z is plotted along the target cross-section surface coordinate s [1] for an inboard (a) and an outboard cross-section (b).

4 Conclusions

The test rig boundary conditions and the structural response were compared for two sub-component test configurations, an inboard and an outboard cross-section to assess the scalability of the proposed test setup.

It is shown that the actuator work W is larger by factor of 5.8 for the inboard compared to the outboard cross-section while the force F is larger by a factor of 3.6, which makes a relative contribution of 62 %. It is rather favorable to have a displacement dominated work, because the ball joints are the design critical components in the proposed test setup. The required actuator work and resulting force at the ball joints depend on the geometric and structural properties, i. e. the inclination angle θ_f between the load axis and the elastic axis, the ratio between bending and axial stiffness expressed by the radius of gyration, as well as the distance of the centroids of full and cut cross-section. For economic reasons, we propose: (a) to minimize the loads at the ball joints by tilting the specimen within the test rig and (b) to reduce the distance between the full and cut-cross section while keeping the radii of gyration low, i. e. by either choosing a reasonable span-wise cut, or by adding material or a springs connected in parallel to the specimen.

The validation of analytical and finite element models has shown good agreement with experimental results. The verification of the analytical model has shown slight deviations for the inboard cross-section compared to the outboard cross-section. A more advanced analytical model than the used model on the basis of Euler-Bernoulli theory is required to capture the response of such a curved thin-walled structure. For the purpose of the setup design, however, the used beam model is sufficient.

Acknowledgements

We acknowledge the support of the European Commission's Seventh Framework Programme within the IRPWind project (609795) and the support within the Future Concept Fatigue Strength of Rotor Blades project granted by the German Federal Ministry for Economic Affairs and Energy (BMWi) (0325939) and the Senator for Health, Environment and Consumer Protection of the Free Hanseatic City of Bremen within the ERDF programme Bremen 2014-2020 (201/PF_IWES_Zukunftskonzept_Betriebsfestigkeit_Rotorblätter_ Phase I).

References

[1] Rosemeier, M., Massart, P., and Antoniou, A.: Tailoring the design of a trailing edge sub-component test, https://doi.org/10.5281/zenodo.153837, presented at 3rd annual IRPWind conference in Amsterdam, the Netherlands, 19-20th September 2016.
[2] Lahuerta, F., de Ruiter, M. J., Espinosa, L., Koorn, N., and Smissaert, D.: Assessment of wind turbine blade trailing edge failure with sub-component tests, in: Proceedings of 21st International Conference on Composite Materials, 2017.
[3] Branner, K., Berring, P., and Haselbach, P.: Subcomponent testing of trailing edge panels in wind turbine blades, in: Proceedings of 17th European Conference on Composite Materials, 2016.
[4] Rosemeier, M., Basters, G., and Antoniou, A.: Benefits of sub-component over full-scale blade testing elaborated on trailing edge bond line design validation, Wind Energy Science Discussions, DOI: 10.5194/wes-2017-35, 2017.
[5] Cotrell J et al. Base excitation testing system using spring elements to pivotally mount wind turbine blades, United states patent, US8601878, 2013.
[6] Richards W D et al. Fatigue testing of wind turbine blade, UK patent application, GB2548589, 2017.
[7] Blasques, J. and Bitsche, R.: An efficient and accurate method for computation of energy release rates in beam structures with longitudinal cracks, Engineering Fracture Mechanics, 133, 56–69, 2015.
[8] Blasques, J., Bitsche, R., Fedorov, V., and Lazarov, B.: Accuracy of an efficient framework for structural analysis of wind turbine blades, Wind Energy, 2015.
[9] Blasques, J. P.: Multi-material topology optimization of laminated composite beams with eigenfrequency constraints, Composite Structures, 111, 45–55, 2014.
[10] Blasques, J. P. and Stolpe, M.: Multi-material topology optimization of laminated composite beam cross sections, Composite Structures, 94, 3278–3289, 2012.

[11] Swanson, J. A.: ANSYS Mechanical APDL, version 15.0, 2014.
[12] Zahle, F., Réthoré, P.-E., Graf, P., Dykes, K., and Ning, A.: FUSED-Wind v0.1.0, DOI: 10.5281/zenodo.13899, 2015.
[13] Euler, L.: Solutio problematis de invenienda curva, quam format lamina utcunque elastica in singulis punctis a potentiis quibuscunque sollicitata, 1728.
[14] Gere, J.: Mechanics of materials, 6th edition, 2004.